



## Full Length Article

# Effect of light alkanes and aromatics on decalin dehydrogenation over noble metal catalysts: A new strategy for the development of naphthalene-based LOHCs

Eva Díaz, Pablo Rapado-Gallego, Salvador Ordóñez\*

Catalysis, Reactors and Control Research Group (CRC), Department of Chemical and Environmental Engineering, University of Oviedo, Julián Clavería s/n, 33006 Oviedo, Spain



## ARTICLE INFO

## Keywords:

Hydrogen chemical storage  
Dehydrogenation kinetics  
Kinetic model  
Carbochemistry

## ABSTRACT

The use of the naphthalene/decalin pair as a liquid organic hydrogen carrier has gained increasing interest due to its high hydrogen loading capacity and industrial availability. However, a major challenge in its application is the fact that naphthalene is a solid at ambient conditions, leading to the solidification of the unloaded organic carrier. To address this limitation, small amounts of light organics, such as monoaromatics or cycloalkanes, can be added. In this study, we investigated the dehydrogenation of decalin over various supported precious catalysts (Pt, Pd, Rh, Ru; supported on both activated carbon and alumina) in a stirred batch reactor at 200 °C. Initial experiments were conducted with pure decalin, and we found that Pt/C provided the best performance. Subsequently, we studied the dehydrogenation of decalin in mixtures with different solvents (cyclohexane, methylcyclohexane, benzene, and toluene in the concentration range of 10–40% of the light hydrocarbon). Our results show that the addition of cycloalkanes did not affect the main reaction, while aromatic compounds exhibited weak inhibition. A Langmuir-Hinshelwood kinetic model has been proposed for predicting this behavior, taking into account the significant inhibitory impacts of naphthalene and, when present, the aromatic additive.

## 1. Introduction

Decarbonizing industrial processes is very challenging under the new environmental regulations, such as the European Green Deal [1]. Hydrogen could be an efficient energy carrier to achieve climate neutrality in the EU by 2050, as it only produces water when converted into energy. However, the low volumetric density of hydrogen hinders its current use in mobile and stationary applications [2]. Liquid organic hydrogen carriers (LOHC) are a promising alternative, as they offer inherent safety and advantages over cryogenic and compression-based strategies [3]. LOHCs consist of pairs of high-boiling point organic molecules that can be catalytically hydrogenated and dehydrogenated [4]. Occasionally, low-melting solids can also be dehydrogenated counterparts. Homocyclic compounds, such as toluene/methylcyclohexane and benzene/cyclohexane, have been proposed as LOHC pairs due to their low cost and high compatibility with existing infrastructures [5]. However, they require high temperatures for dehydrogenation, leading to the concomitant presence of cracking reactions, which hinder the reusability of the loaded/unloaded LOHCs for a

realistic number of cycles [4,6]. Other potential LOHCs include biphenyl/bicyclohexyl, terphenyl/perhydroterphenyl [7] and dibenzyltoluene/perhydrodibenzyltoluene, the last pair being commercialized by Hydrogenious [8]. Another option is naphthalene/decalin ( $\Delta H_{\text{reaction}} = 66.3 \text{ kJ/mol H}_2$ ), which has a high hydrogen capacity (7.3 %) and reduced losses by evaporation during storage, due to the high boiling points: 187–196 °C for trans- and cis-decalin, and 218 °C for naphthalene [9,10]. However, the naphthalene melting point, 80 °C, makes it solid at ambient conditions, requiring mixtures with light compounds to maintain a liquid state.

Several works dealing with decalin dehydrogenation have been published, especially using platinum or palladium as catalytic active phase [6,9,11,12], although nickel [10], with lower cost, was also tested. Concerning the supports, activated carbon is the preferred [13–14], as side reactions (ring opening, cracking, or isomerization) are reported to be promoted with more acidic supports, such as mesoporous alumina [6,15,16]. Comparing Pd and Pt, Kim et al. [11] reported that Pt is more active for the decalin to tetralin conversion, whereas Pd is more active for the tetralin to naphthalene reaction. Likewise, concerning

\* Corresponding author.

E-mail address: [sordonez@uniovi.es](mailto:sordonez@uniovi.es) (S. Ordóñez).<https://doi.org/10.1016/j.fuel.2023.129168>

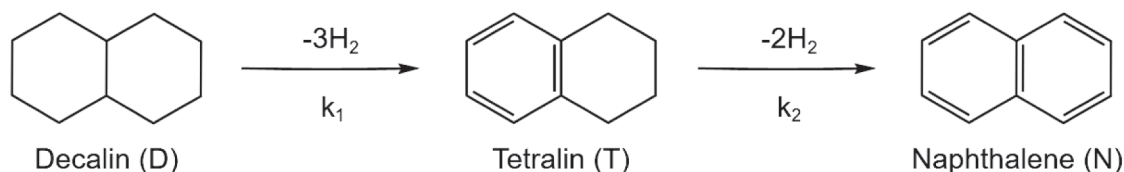
Received 25 April 2023; Received in revised form 22 June 2023; Accepted 2 July 2023

Available online 7 July 2023

0016-2361/© 2023 The Author(s). Published by Elsevier Ltd. This is an open access article under the CC BY-NC-ND license (<http://creativecommons.org/licenses/by-nc-nd/4.0/>).

**Table 1**  
Main physicochemical properties of the catalysts used in this work.

Catalyst	Manufacturer	Metal loading (wt %)	S <sub>BET</sub> (m <sup>2</sup> /g)	Dispersion (%)	dp (nm)	Reference
Pt/C	Prepared according to [19]	0.5	1716	21.3	4.7	[19]
Pt/C	Doduco	5	778	7.3	15.5	[20]
Pt/Al <sub>2</sub> O <sub>3</sub>	Engelhard	0.5	116	23.9	4	[21]
Pt/Al <sub>2</sub> O <sub>3</sub>	Engelhard	5	168	25	4.5	[22]
Pd/Al <sub>2</sub> O <sub>3</sub>	Engelhard	0.5	92	34	3.3	[23]
Rh/Al <sub>2</sub> O <sub>3</sub>	Engelhard	0.5	117	35	2.9	[24]
Ru/Al <sub>2</sub> O <sub>3</sub>	Engelhard	0.5	118	28	4	[24]



**Scheme 1.** Simplified reaction mechanism for decalin dehydrogenation reactions.

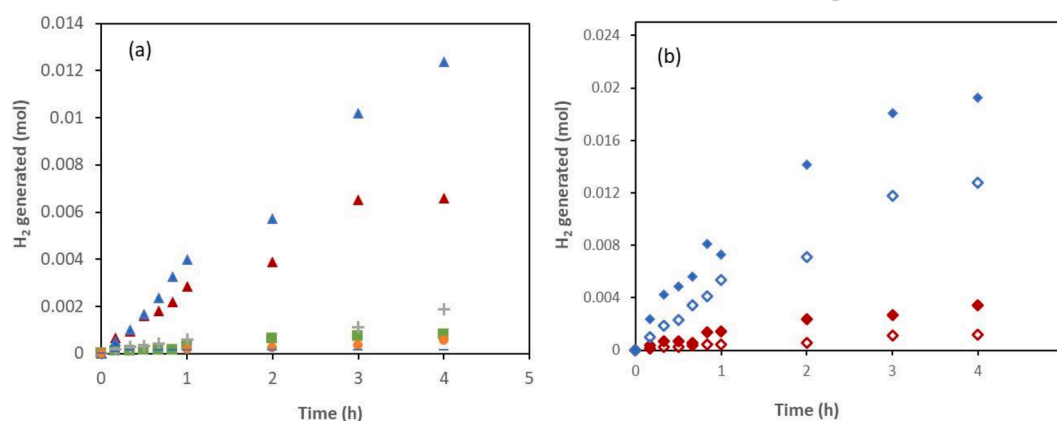


**Fig. 1.** Hydrogen evolution during decalin dehydrogenation at 200 °C as function of reaction time: a) H<sub>2</sub> generated on 1.5 g alumina supported catalysts [0.5 wt% Pt/Al<sub>2</sub>O<sub>3</sub> (▲); 5 wt% Pt/Al<sub>2</sub>O<sub>3</sub> (▲); 0.5 wt% Pd/Al<sub>2</sub>O<sub>3</sub> (■); 0.5 wt% Rh/Al<sub>2</sub>O<sub>3</sub> (●); 0.5 wt% Ru/Al<sub>2</sub>O<sub>3</sub> (■); 0.5 wt% Pt/Al<sub>2</sub>O<sub>3</sub> + 0.5 wt% Pd/Al<sub>2</sub>O<sub>3</sub> (+)]; b) H<sub>2</sub> generated on carbon supported catalysts [0.5 g, 0.5 wt% Pt/C (◇); 1.5 g, 0.5 wt% Pt/C (◆); 0.5 g, 5 wt% Pt/C (◇); 1.5 g, 5 wt% Pt/C (◆)].

dehydrogenation rates, decalin dehydrogenation is slower than tetralin dehydrogenation [17,18].

To our knowledge, the use of the decalin/naphthalene pair for hydrogen chemical storage has been poorly investigated, mainly because the resulting product of dehydrogenation, naphthalene, is solid under typical conditions. However, it is worth noting that both naphthalene and decalin exhibit complete miscibility with aromatic solvents, as well as their hydrogenated counterparts (cycloalkanes). In this research, we aim to address these gaps by conducting a comprehensive analysis of the kinetics of decalin dehydrogenation in both pure form and mixtures with organic solvents, which promote the solubilization of the resulting naphthalene. Our approach involves using noble metal active phases supported by activated carbon and alumina, since these are the most common and widely available catalysts using for catalytic dehydrogenation of pure LOHCs.

## 2. Experimental

### 2.1. Dehydrogenation reaction

Decalin dehydrogenation experiments were conducted in a glass stirred batch reactor (50 mL) at boiling conditions (200 °C, atmospheric pressure). In order to avoid the loss of organic molecules, the reactor is

connected to an open-ended water-chilled condenser, operating under reflux conditions. Unless otherwise stated, magnetic stirring at 1000 rpm was applied in all the experiments. Decalin (cis- and trans- mixture, >99 %) was purchased from Sigma-Aldrich, as well as tetralin and naphthalene (99 %). Typically, 20 mL of liquid, pure decalin or the corresponding mixture, were introduced in the reactor, that was heated to the desired temperature using a commercial heat-transfer fluid. The reaction begins with the introduction of either 0.5 or 1.5 g of previously reduced catalyst (4 h at 300 °C for Pt catalysts and 250 °C for the other catalysts, in flowing hydrogen gas), Table 1, and reaction was conducted for either 4 or 8 h. A fraction of 80–100 μm was selected unless otherwise stated. Previously, a blank experiment was carried out observing null tetralin or naphthalene production. Initially and periodically, samples of 0.5 mL we extracted, filtered with a syringe filter (0.1 μm) and dissolved in 4 mL n-hexane to analyzed by a gas chromatography in a Shimadzu GC-2010 equipped with a FID detector (30 m long CP-Sil 8 CB capillary column). Calibration of reactant and products was done using commercial standards. Conversion (x) was calculated from the difference between the initial and final decalin concentration (Eq. (1)), whereas selectivity (S) to each product was calculated as the ratio of the moles converted to the product considered over the total moles converted (Eq. (2)). Finally, the yield (η) of the different compounds was calculated by Eq. (3). Concerning the hydrogen production, it was

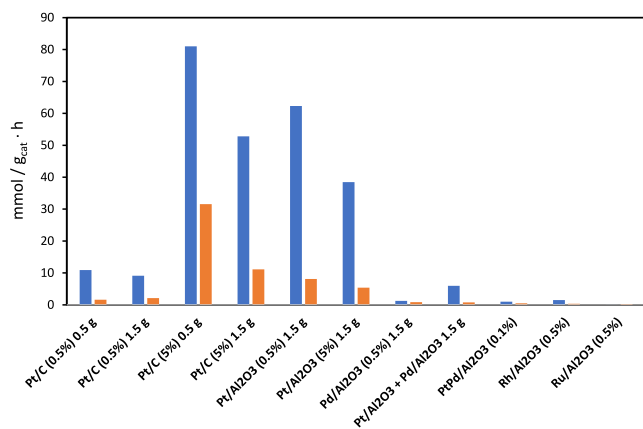


**Fig. 2.** Summary of the tetralin (blue) and naphthalene (orange) productivities (expressed as mmol of product obtained by time and catalyst loading) obtained with the different catalysts studied in this work ( $T = 200\text{ }^{\circ}\text{C}$ ; pure decalin as reactant, 4 h reaction time). (For interpretation of the references to colour in this figure legend, the reader is referred to the web version of this article.)

calculated from tetralin and naphthalene formed according to the reaction stoichiometry, [Scheme 1](#).

$$x (\%) = \left(1 - \frac{C_i}{C_0}\right) \cdot 100 \quad (1)$$

$$S_i (\%) = \frac{n_i \cdot C_i}{\sum (n_i \cdot C_i)} \cdot 100 \quad (2)$$

$$\eta_i = \chi_i \cdot S_i \quad (3)$$

## 2.2. Catalysts characterization

The pore properties and specific surface area were measured by a Micromeritics ASAP 2020 nitrogen adsorption apparatus at 77 K. High-resolution transmission electron microscopy (HRTEM, JEOL JEM2100F) analyses of the fresh materials were carried out to determine the nanoparticle size and distribution, as well as the metal dispersion.

## 3. Results and discussion

### 3.1. Decalin dehydrogenation on different catalysts

Hydrogen releases during decalin dehydrogenation experiments performed at  $200\text{ }^{\circ}\text{C}$  are shown in [Fig. 1](#). All the curves show an initial fast  $\text{H}_2$  evolution, which in the case of carbon supported catalysts reaches a maximum after three hours, and further decrease in the hydrogen release, [Fig. 1b](#). From comparison between both supports it is observed that the reaction proceeds slower for alumina support, whereas Pt is the active phase providing the highest reaction rates ([Fig. 1a](#)), although Pd also presents a significant activity. Catalyst activity is nearly negligible for the other metallic phases considered (Ru, Rh), [Fig. 1a](#). From these results, two Pt catalysts (0.5 and 5%) were tested, observing that at 3 h the 0.5% catalyst stopped producing  $\text{H}_2$ , while the 5% catalyst continued with the same rate. The effect of both catalyst weight and Pt loading was also studied for activated carbon, [Fig. 1b](#). For the lowest catalyst loadings, 0.5%, an upward trend in hydrogen formation is observed throughout the 4 h of reaction, while its formation is interrupted at three hours for the 5% Pt catalyst. From the comparison of the  $\text{H}_2$  formation rate at three hours, it can be deduced that tripling the mass of the 0.5% Pt catalyst practically triples the  $\text{H}_2$  formation rate (from 0.5 mmol/h to 1.4 mmol/h), while for the 5% Pt catalyst, it advances from 5.5 mmol/h to 9.5 mmol/h, thus, it is barely multiplied by 1.7. What is

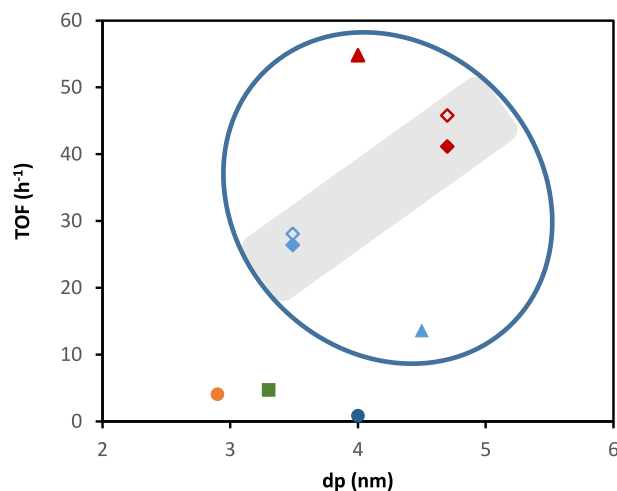


**Fig. 3.** Decalin dehydrogenation TOF evolution at  $200\text{ }^{\circ}\text{C}$  with crystallite size. Shadow area corresponding to Pt/C catalysts, whereas blue line includes the Pt catalysts. Symbols: 0.5 g, 0.5 wt% Pt/C ( $\blacklozenge$ ); 1.5 g, 0.5 wt% Pt/C ( $\blacklozenge$ ); 0.5 g, 5 wt% Pt/C ( $\blacklozenge$ ); 1.5 g, 5 wt% Pt/C ( $\blacklozenge$ ); 1.5 g, 0.5 wt% Pt/ $\text{Al}_2\text{O}_3$  ( $\blacktriangle$ ); 1.5 g, 5 wt% Pt/ $\text{Al}_2\text{O}_3$  ( $\blacktriangle$ ); 1.5 g, 0.5 wt% Pd/ $\text{Al}_2\text{O}_3$  ( $\blacksquare$ ); 1.5 g, 0.5 wt% Rh/ $\text{Al}_2\text{O}_3$  ( $\bullet$ ); 1.5 g, 0.5 wt% Ru/ $\text{Al}_2\text{O}_3$  ( $\bullet$ ). (For interpretation of the references to colour in this figure legend, the reader is referred to the web version of this article.)

more, for the catalysts mass loading of 0.5 g, the increase in Pt content from 0.5 to 5%, multiplied the  $\text{H}_2$  production of  $\text{H}_2$  by 10, whereas for 1.5 g mass loading, it no longer follows the proportion.

Liquid products yield is plotted in [Fig. 2](#), evidencing that Pt catalysts present the highest yield for both products, in agreement with hydrogen production reported in [Fig. 1](#). Likewise, the tetralin/naphthalene ratio is a key parameter for catalyst comparison, since the activation energy for dehydrogenation of decalin to tetralin is higher than the corresponding to tetralin dehydrogenation to naphthalene [[16,25](#)].

The mechanical mixture of Pd/ $\text{Al}_2\text{O}_3$  and Pt/ $\text{Al}_2\text{O}_3$  presents a poor behaviour in comparison with Pt catalyst, although improved with respect to noble metals different from Pt. This catalysts mixture was tested to reach higher naphthalene selectivities, since Pt is preferred in the conversion of decalin to tetralin whereas Pd in the conversion of tetralin to naphthalene [[11](#)], however the amount of Pt seems to be the limiting factor. Concerning the role of support, carbon supported catalysts present increased yields, in agreement to [Fig. 1](#). In fact, the rate of  $\text{H}_2$  production over Pt/carbon catalysts was estimated to double Pt/ $\text{Al}_2\text{O}_3$  one [[13](#)].

To compare the intrinsic activity of the catalysts, results are expressed in terms of turnover frequencies (TOF), defined as molecule of decalin converted by exposed metal atom and time ([Fig. 3](#)). A marked increase of TOF with crystallite size is observed for Pt catalysts, being this trend more marked for the Pt/ $\text{Al}_2\text{O}_3$  catalyst.

The observed TOF evolution with  $d_p$  for Pt catalysts contrast with previous works where dehydrogenation reactions were described as structure sensitive, exhibiting a negative correlation between dehydrogenation ability, of decalin and dodecahydro N-ethylcarbazole, and the metal particle size [[15,26](#)]. However, in other works about cyclohexane and dodecahydro N-ethylcarbazole dehydrogenation [[27,28](#)], a volcano shaped trend of TOF with metal crystallite size is observed, centered at 1.9 and 9 nm, respectively, being justified by the different reactivities of edges and terraces of the metal crystallite. Thus, small molecules are more sensible to the interaction with surface irregularities (as crystallite edges, more concentrated at the lowest crystal sizes), leading to a catalytic overperforming. As molecule size increases, interaction of this molecule with these irregular sites is hindered, and molecule-metal interaction is controlled with metal surface availability, leading to a

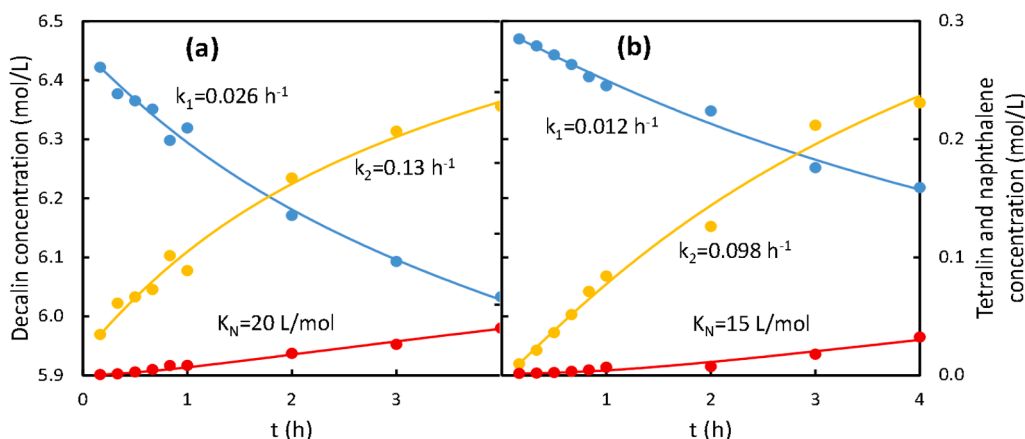


Fig. 4. Comparison between experimental (dots) and fitted results (lines) in the dehydrogenation of decalin at 200 °C with 1.5 g of: (a) Pt 5 wt% supported on activated carbon, (b) Pt 5 wt% supported on alumina. Results correspond to decalin (●), tetralin (●) and naphthalene (●).

positive effect of crystallite diameter on reactor performance [29].

The best dehydrogenation performance (in terms of TOF values), exhibited by 0.5 % Pt/C and 0.5 % Pt/Al<sub>2</sub>O<sub>3</sub>, corresponds to a crystallite size of the interval 4–4.7 nm. The flat configuration of the decalin molecule could explain the better performance of the larger crystallites, in contrast to cyclohexane, a much smaller molecule, or dodecahydro N-ethyl-carbazole which is larger but has ethyl group out of the ring plane. It should be noted that crystalline morphology is not the only explanation for these effects, since 5 % Pt/Al<sub>2</sub>O<sub>3</sub> catalyst present a largely poorer performance, in spite of its similar metal dispersion.

Considering these preliminary results, subsequent experiments were performed only with 5 % Pt/C (providing the best results on terms of conversion and selectivity) and 5 % Pt/Al<sub>2</sub>O<sub>3</sub> for comparison purposes, since competitive adsorption effects can also depend on support chemistry.

### 3.2. Kinetics of decalin dehydrogenation

According to the literature, the dehydrogenation of decalin includes several reversible reactions: tetralin formation from both *cis*-decalin and *trans*-decalin; conversion of tetralin to naphthalene; and isomerization of *cis*- and *trans*-decalins [10]. In this work, the contribution of both decalin isomers were considered together, thus, the reaction could be described according to Scheme 1.

Reaction data was preliminary fitted to single power-law models (first and second order reactions, both considering reversible and irreversible reaction for both steps), these models not providing good fit of the experimental results. Thus, a Langmuir-type equation compatible with a first order reaction, was proposed, in which the inhibition effect of the aromatic products is considered. These Langmuir approaches are widely used and accepted for modelling catalytic reactions in presence inhibition effects caused by reactants, products or spectator species. These assumptions are compatible with previous works [25,30], which suggest a non-negligible inhibitory effect of the aromatic intermediates, being usually stronger the interaction of a polycyclic molecule as the number of aromatic rings increases. The same authors also suggest that these effects are negligible with completely or partially hydrogenated polyaromatics (as decalin and tetralin, respectively).

Likewise, the reversibility of both reactions was also tested, observing total irreversibility in the decalin dehydrogenation reaction, which agrees with the irreversibility observed in the tetralin hydrogenation reaction by other authors [31]. Regarding the dehydrogenation of tetralin to naphthalene, although several authors consider that this step could be reversible, kinetic constant for the reverse reaction was in all the cases one order of magnitude lower than the forward reaction.

This fact is in a good agreement with the main results published on naphthalene hydrogenation using precious noble metal catalysts. Reported conditions for obtaining significant hydrogenation rates are larger catalyst loadings (most of the times with fixed bed reactors) and higher operation pressures (50–70 bar) [32–34].

Therefore, both reactions have been considered as irreversible in the present work (Eqs. (4)–(6)).

$$\frac{dC_D}{dt} = \frac{-k_1 C_D}{1 + K_N C_N} \quad (4)$$

$$\frac{dC_T}{dt} = \frac{k_1 C_D - k_2 C_T}{1 + K_N C_N} \quad (5)$$

$$\frac{dC_N}{dt} = \frac{k_2 C_T}{1 + K_N C_N} \quad (6)$$

where  $C_D$ ,  $C_T$  and  $C_N$  represent decalin, tetralin, and naphthalene concentrations, respectively, and  $k_1$  and  $k_2$  are the apparent reaction rate constants and  $K_N$  is the naphthalene adsorption constant. Considering additional inhibition terms for tetralin or decalin adsorption do not provide better fits despite using a larger number of model parameters.

Before further proceeding with kinetic modelling, the absence of both external and internal mass transfer effects must be ensured. As the reaction is performed in a boiling liquid, hydrogen is rapidly removed from reaction medium, being negligible the effect of this gas in the mass transfer. Reactions are performed in pure decalin, at low conversions (<10%), and the reactions are irreversible. Thus, external reactant film gradients will be negligible and the external mass transfer effects can be discarded. In good agreement with this fact, similar results were obtained when working without stirring (decalin boiling conditions) and when working with a magnetic stirrer at different spinning velocities (500–1500 rpm, for 5 % Pt/C).

Concerning to the internal mass transfer effects, it should be noted that decalin diffusion through the pore could be limiting, especially for Pt/C (smaller pore diameter and high catalytic activity). So, this catalyst has been selected for a more detailed study of internal mass transfer (5 % Pt, experiment performed at 200 °C). As the reaction takes place at liquid phase conditions, diffusion effects depend only on molecular diffusion. For estimating molecular diffusion coefficients, it should be noted that reaction is performed in an almost pure liquid reactant media. Thus, self-diffusion coefficient of decalin at reaction conditions was estimated using the Stokes-Einstein approximation ( $1.8 \times 10^{-9} \text{ m}^2/\text{s}$ ). Effective diffusion coefficient was calculated considering reported values of catalyst particle porosity and tortuosity for these particles ( $\epsilon =$

**Table 2**  
Properties of decalin solvents [37].

	Benzene	Cyclohexane	Toluene	Methyl-cyclohexane
Napthalene solubility at 25 °C (g/L)	809	450	673	430
Melting point (°C)	5	6	-95	-127
Boiling point (°C)	80	80	110	74

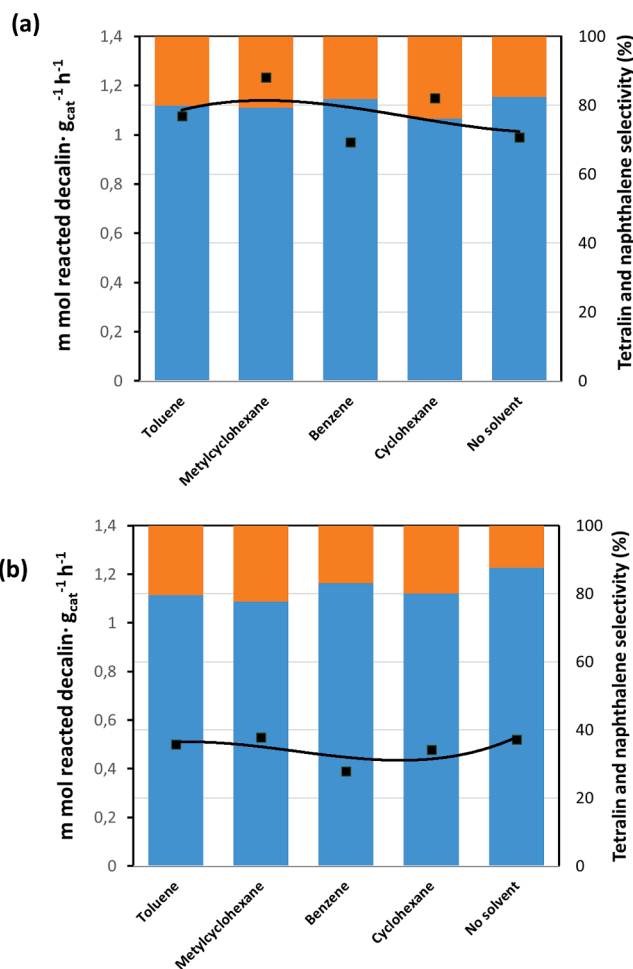


**Fig. 5.** Conversion (%) and tetralin (blue) and naphthalene (orange) selectivity for decalin dehydrogenation on 10 % vol. solvent, at 200 °C, 1.5 g catalyst and after 4 h reaction time: (a) Pt 5 wt% supported on activated carbon, (b) Pt 5 wt % supported on alumina. (For interpretation of the references to colour in this figure legend, the reader is referred to the web version of this article.)

0.3, and  $\tau = 4$ , respectively, which lead to an effective diffusivity of  $1.8 \times 10^{-10} \text{ m}^2/\text{s}$ ). According to these assumptions, and applying the Wheeler-Weisz criterium, the reaction is clearly controlled by the chemical reaction (Weisz number,  $We = 10^{-4} \ll 0.1$ ). Accordingly, experiments repeated with lower particle size (50–80  $\mu\text{m}$  vs 80–100  $\mu\text{m}$ ) provide similar results in terms of activity and selectivity.

The MATLAB function “lsqcurvefit” using the Levenberg-Marquardt algorithm was used for fitting the experimental results. The fitting of the unknown parameters from the model is accomplished by the least-square method. The coefficient of determination was calculated with the MATLAB function “rsquare”.

According to the highest activity observed for the 5 % Pt/C catalyst, this catalyst, as well as 5 % Pt/Al<sub>2</sub>O<sub>3</sub>, for comparative purposes, have been selected to carry out the kinetic studies. The kinetic constants, and

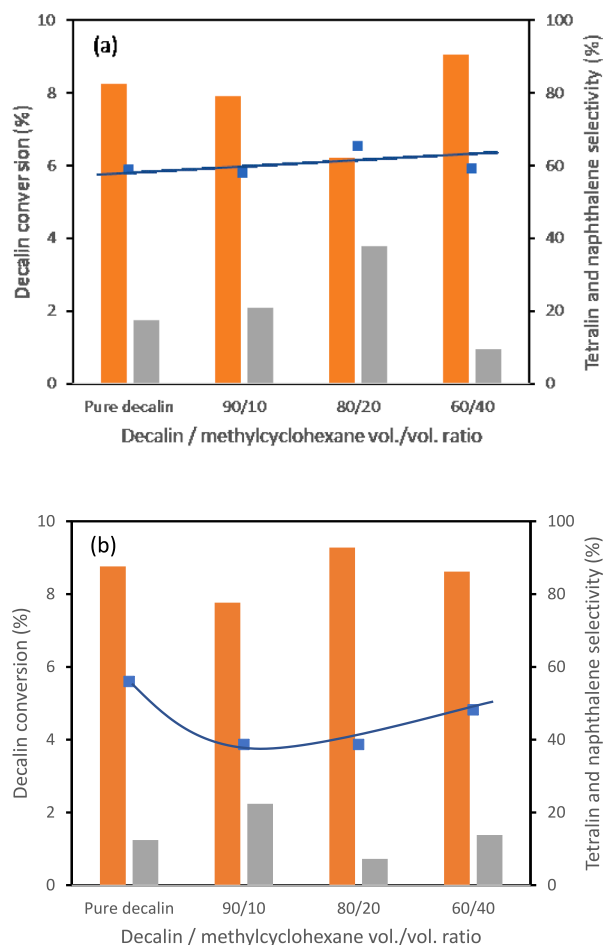


**Fig. 6.** Decalin conversion (blue) and tetralin (orange) and naphthalene (grey) selectivity at different decalin:methylcyclohexane vol./vol. ratio on: (a) 5 wt% Pt/C catalyst, (b) 5 wt% Pt/Al<sub>2</sub>O<sub>3</sub> catalyst, 1.5 g catalyst, at 200 °C, 4 h. (For interpretation of the references to colour in this figure legend, the reader is referred to the web version of this article.)

the goodness of the fit are shown in Fig. 4. The best performance of the carbon-supported catalysts cannot be explained neither in terms of the metal dispersions (as previously discussed) nor in terms of the role of the support reactivity. This last point can be discarded because both the weakness of the acidity of the alumina acid sites and the absence of cracking or ring-opening products among the reaction products. These reactions have been observed in the literature in other dehydrogenation reactions [35]. Thus, the positive role of carbon-supported catalysts seems to be related with a promotional effect of the high-surface area support on the decalin adsorption, increasing the local concentration of reactants and products on the crystallite vicinity.

Kinetic constants evidenced that decalin dehydrogenation is slower than the equivalent tetralin reaction, and both reaction rates are more favoured on Pt/C catalyst, especially the first one. Likewise, the inhibitory effect of naphthalene is higher on carbon supported catalysts ( $K_N$ ), suggesting that  $\pi$ - $\pi$  interactions between the naphthalene and the graphitic planes of the activated carbon enhances the chemisorption of this chemical on the metal active sites. The same effect can also justify the higher reactivity of the carbon-based catalysts in comparison with the alumina-supported ones.

A comparison of our kinetic constants with those obtained from published data is useful for contrasting the performance of our catalysts and reaction system with the state of the art. Although this comparison is

**Table 3**

Estimated kinetic parameters for decalin dehydrogenation from mixtures. Regression coefficients &gt; 0.88.

Solvent	5 % Pt /C				5 % Pt /Al <sub>2</sub> O <sub>3</sub>			
	$k_1$ (h <sup>-1</sup> )	$k_2$ (h <sup>-1</sup> )	$K_N$ (L/mol)	$K_L$ (L/mol)	$k_1$ (h <sup>-1</sup> )	$k_2$ (h <sup>-1</sup> )	$K_N$ (L/mol)	$K_L$ (L/mol)
–	0.026	0.13	20	–	0.012	0.098	15	–
10 % Benzene	0.025	0.20	41	0.30	0.008	0.11	55	43
10 % Cyclohexane	0.024	0.19	49	0.00	0.009	0.15	57	3.3
10 % Toluene	0.023	0.19	25	0.42	0.012	0.17	29	33
10 % Methylcyclohexane	0.026	0.17	28	0.00	0.009	0.22	23	4.0

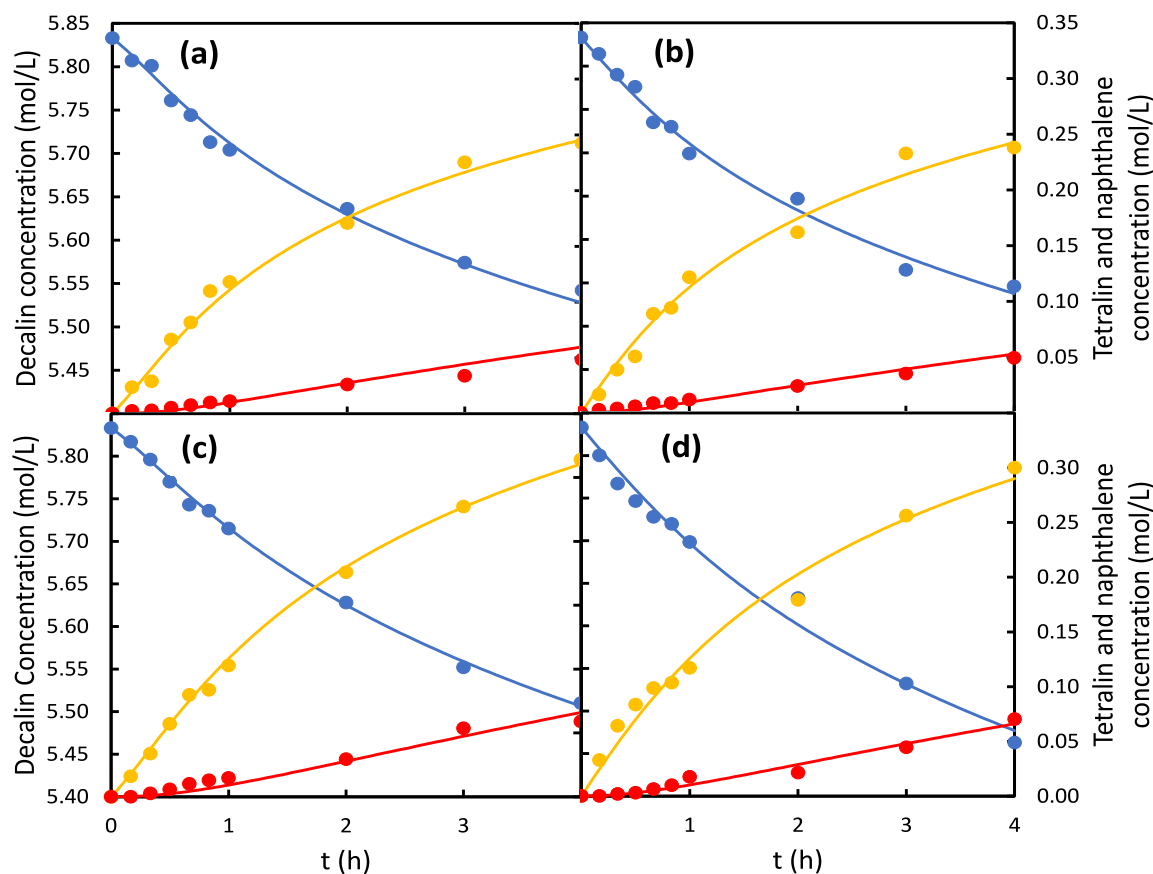


**Fig. 7.** Comparison between experimental (dots) and fitted results (lines) in the dehydrogenation at 200 °C with 1.5 g of 5 % Pt/C of 90 % decalin/10 % the following solvents: (a) benzene, (b) cyclohexane, (c) toluene, and, (d) methylcyclohexane. Results correspond to decalin (●), tetralin (●) and naphthalene (●).

not straightforward (different reactor configuration, catalyst loadings and operation conditions), our results are congruent with the obtained with other research groups. For example, Kalenchuk et al. [36], studying decalin dehydrogenation in a fixed bed at 320 °C (3 %Pt/C) propose first-order kinetic constants of 0.03 h<sup>-1</sup> for *cis*-decalin and 0.416 h<sup>-1</sup> for *trans*-decalin. The equivalent parameter for our case (initial conditions, neglecting the influence of naphthalene) leads to a first order kinetic constant of 0.026 h<sup>-1</sup> (200 °C, 5 %Pt/C). Looking at batch reactors, data provided by Hodoshima et al. [9] leads to a kinetic constant of 0.2 h<sup>-1</sup> at 210 °C, but working with a catalyst concentration of 0.3 g/mL, whereas we are working at 200 °C with a catalyst concentration of 0.075 g/mL of a similar catalyst (5% Pt/C).

### 3.3. Decalin dehydrogenation in presence of solvents

Decalin dehydrogenation yields both tetralin and naphthalene, being the product formed in the second reaction solid at ambient temperature,

hindering its application as LOHC (storage and transport of the LOHC is easier working with liquids). To overcome this problem, adding an organic solvent can allow to work with liquid streams. The situation is even better if this solvent can also storage hydrogen. At this point, the influence of temperature on naphthalene solubility in different solvents was previously studied between -25 and 25 °C [37], with the aim to cover the most common temperatures on the European continent, from the Nordic countries with temperatures around -20 °C in winter to the warmest ones, being especially critical to the solubility the lowest ones. The naphthalene solubility is maximum for benzene, followed by toluene, solvents traditionally used in the industry. However, the benzene melting point, 5 °C, could limit this application. Considering that decalin dehydrogenation is carried out at much higher temperatures, both compounds as well as their hydrogenated pairs, cyclohexane and methylcyclohexane, with H<sub>2</sub> content of 7.13 and 6.16 wt%, respectively, where essayed as decalin solvents. Their properties are summarized in Table 2.

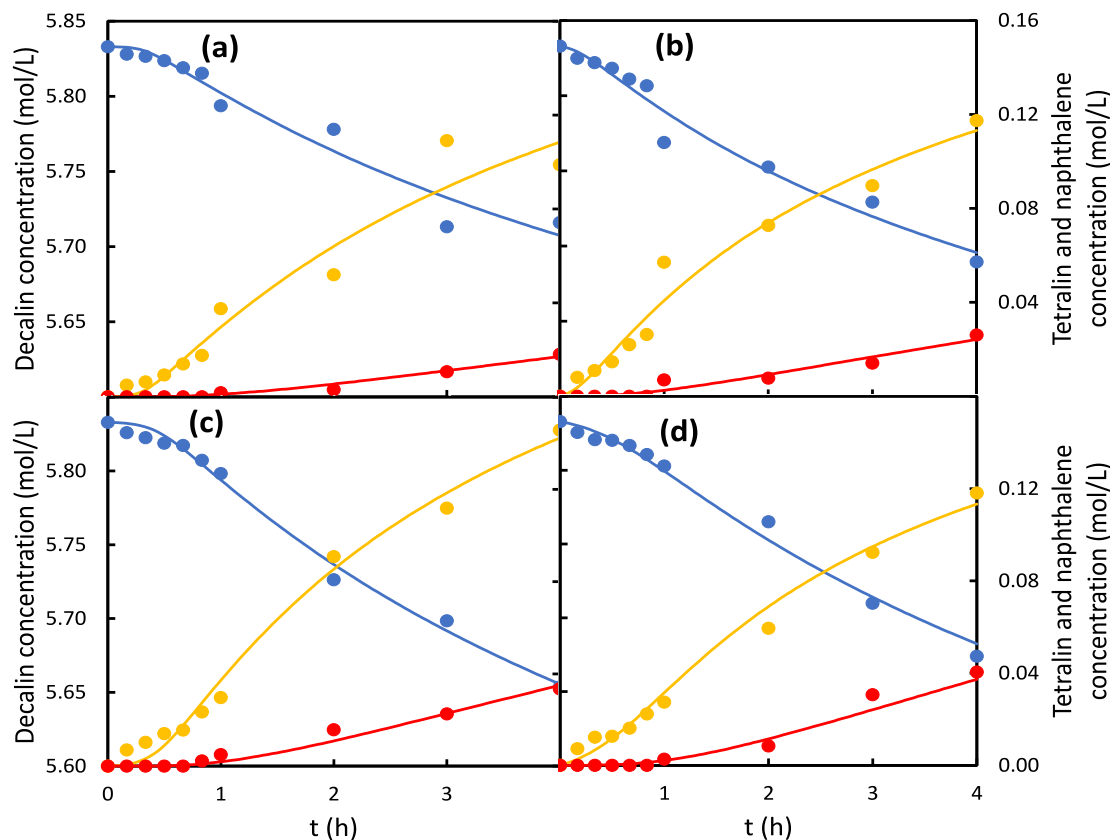


**Fig. 8.** Comparison between experimental (dots) and fitted results (lines) in the dehydrogenation at 200 °C with 1.5 g of 5 % Pt/Al<sub>2</sub>O<sub>3</sub> of 90 % decalin/10 % the following solvents: (a) benzene, (b) cyclohexane, (c) toluene, and, (d) methylcyclohexane. Results correspond to decalin (●), tetralin (●) and naphthalene (●).

The effect of these solvents in decalin dehydrogenation was initially considered from mixtures containing 90 % decalin and 10% solvent, by volume. Reactions were conducted with both 5 wt% Pt/C and 5 wt% Pt/Al<sub>2</sub>O<sub>3</sub> catalysts, 1.5 g, 8 h and at 200 °C.

Reaction behaviour of decalin dehydrogenation in solvents after 4 h are depicted in Fig. 5, whereas temporal profiles are discussed in the next section, where a kinetic model is proposed. For both catalysts, it is observed that the presence of solvent in the media scarcely influences the selectivity towards both the intermediate and final reaction product, being more active the Pt/C catalysts. Likewise, although decalin conversion varies in a fairly narrow interval, is slightly higher in the presence of hydrogenated solvents, matching the conversion to the reaction of pure decalin, whereas the addition of aromatics to decalin would decrease the decalin conversion. This fact is related to the strongest adsorption of the aromatic structure, [38], and is in a good agreement with the abovementioned inhibition effect of the naphthalene in this reaction. Dehydrogenation of cyclohexane or methylcyclohexane is not observed, in agreement with the higher temperatures usually necessary to carry out the reaction for similar catalysts [39].

Considering that from the studied solvents, methylcyclohexane offers the most promising behavior, the influence of methylcyclohexane content was deeply studied, Fig. 6. Although a pernicious effect of methylcyclohexane is evidenced on Pt/Al<sub>2</sub>O<sub>3</sub> catalyst, attending both to decalin reactivity and selectivity of the final reaction product, a beneficial effect is observed for Pt/C catalyst, especially for 60:40 ratio. These results suggest that controlled addition of these light chemicals can improve the physical properties of the LOHC with a minor effect on the dehydrogenation performance.

### 3.4. Kinetic modelling of decalin dehydrogenation in mixtures

Kinetics of decalin dehydrogenation in presence of benzene, toluene, and the compounds resulting from its dehydrogenation were described by a Langmuir-type model in an analogous way as pure decalin. In the kinetic modelling, add to naphthalene inhibition, the solvent one was also considered, Eqs. (7)–(9).

$$\frac{dC_D}{dt} = \frac{-k_1 C_D}{1 + K_L C_L + K_N C_N} \quad (7)$$

$$\frac{dC_T}{dt} = \frac{k_1 C_D - k_2 C_T}{1 + K_L C_L + K_N C_N} \quad (8)$$

$$\frac{dC_N}{dt} = \frac{k_2 C_T}{1 + K_L C_L + K_N C_N} \quad (9)$$

where  $C_L$  represents light organic concentration, and  $K_L$  is the adsorption constant of the solvent.

Table 3 summarizes the kinetic constants obtained for dehydrogenation reactions, whereas the goodness of the fit is illustrated in Fig. 7 and Fig. 8.

Kinetic constants of decalin-solvent (90:10 vol./vol.) solutions, Table 3, show that reaction rates are similar to pure decalin, although with some variations. The values of  $k_1$  are very similar for the experiments performed in absence and presence of solvents (within the statistical error for Pt/C, and with minor variations for Pt/Al<sub>2</sub>O<sub>3</sub>). Thus, differences on the reactant conversions are mainly due to inhibition effects caused by the naphthalene or the added solvents, suggesting that the mechanism of the surface reaction (assumed to be rate-controlling step) is essentially the same in all the cases. The analysis of the second

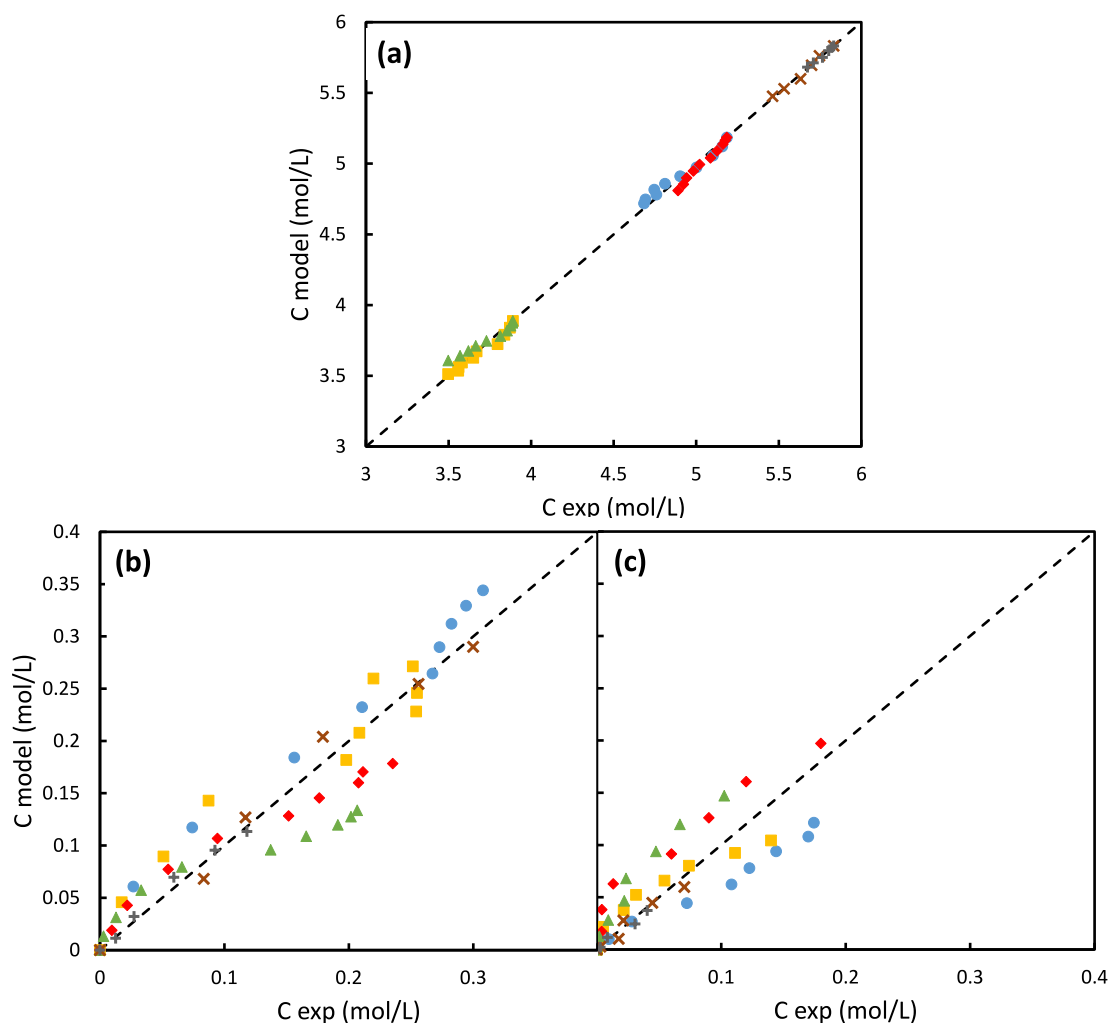


**Fig. 9.** Comparison of the experimental values and model predictions for: (a) decalin, (b) tetralin, and (c) and naphthalene concentrations. Symbols: 5 %Pt/C catalyst, with decalin/methylcyclohexane vol./vol. ratio: 90/10 (X), 80/20 (●) and 60/40 (■); 5 %Pt/Al<sub>2</sub>O<sub>3</sub> catalyst, with decalin/methylcyclohexane vol./vol. ratio: 90/10 (+), 80/20 (◆) and 60/40 (▲).

step is a little bit more complex since the values of  $k_2$  present larger variations. In the case of Pt/C, this kinetic constant is very similar for all the binary mixtures, but significantly higher than the obtained working with pure decalin. In the case of Pt/Al<sub>2</sub>O<sub>3</sub>, the benzene-decalin mixture seems to be a similar behavior than the pure decalin, following in the other cases the same behavior than the observed in the case of Pt/C. These results indicate that the mechanism of the surface reaction is more complex than in the first step, involving adsorbed species and/or intermediate than could act as hydrogen scavengers or donors, promoting the reaction. The distinctive behavior of benzene when using alumina-supported catalysts can be caused by a stronger interaction with alumina Lewis acid sites, minimizing its effect on the metallic sites. In both steps, the reaction seems to be strongly tuned by adsorption effects, both from naphthalene (as previously demonstrated working with pure decalin) and the added solvent. Looking at the effect of the solvent, the trends observed for the inhibition constants follows the expected trend: aromatic solvents (benzene and toluene) present the strongest interaction with the active sites (larger values of  $K_1$ ) for both catalysts, whereas the inhibition effects of cyclohexane and methyl-cyclohexane are less marked, being even negligible for Pt/C. Comparing the value of these inhibition coefficients between both catalysts, the values are always higher for Pt/Al<sub>2</sub>O<sub>3</sub>, which could be justified by the higher surface of the

activated carbon, promoting adsorption on the support far from the active phase and minimizing the interaction with this active phase. In agreement, the solvent inhibition is higher for benzene than toluene, which could be justified attending to its adsorption enthalpies on activated carbons, which is higher for toluene than benzene [40]. The most striking fact of the reported kinetic model is related to the naphthalene adsorption constant. According to a conventional Langmuir-Hinshelwood mechanism, this constant should be similar for a given catalyst, irrespective of the presence of other organics. However, this constant is largely higher in presence of the solvents in all the cases, but being this difference more marked for benzene and cyclohexane (whereas for toluene and MCH the difference is clearly lower). This fact suggests that geometrical constraints are more relevant than electronic effects. The presence of non-alkylated rings seems to promote the adsorption of naphthalene, being this effect attenuated in presence of alkylations.

The model constants obtained for the decalin dehydrogenation reaction in the presence of methylcyclohexane (90/10), Table 3, were used to simulate the results of the dehydrogenation carried out with decalin/methylcyclohexane ratios of 80/20 and 60/40. As can be seen in Fig. 9, the accuracy of the prediction of the experimental values is very high in the case of the reactant and the intermediate product, presenting larger



variations in the case of naphthalene, which is a good agreement with the global lower concentration of this reaction products. This fact suggests that the proposed models can effectively predict the behaviour of the decalin dehydrogenation in presence of other lighter hydrocarbons.

#### 4. Conclusions

Decalin dehydrogenation on several metal active phases and on two supports (activated carbon and alumina) was conducted in this work. Among the studied catalysts, Pt active phase presents the highest yield for both products, tetralin and naphthalene. Concerning the role of support, carbon supported catalysts present increased yields. Although metal crystallite size plays a key role in the catalyst activity, suggesting an optimal value about 4 nm, support surface chemistry effects must be also considered.

In this work, a hypothesis based on the influence of naphthalene solubility on the reaction extension is exposed. In this way, the reaction was studied both as pure decalin and in decalin-solvent (90:10 vol./vol.) solutions with both 5 wt% Pt/C and 5 wt% Pt/Al<sub>2</sub>O<sub>3</sub> catalysts. The concentration evolution of reactant and intermediate and final products in presence of the solvents reveals that the presence of any solvent decrease the conversion of both decalin and tetralin, probably due to the competitive adsorption of H-acceptor and donor molecules on catalytic sites. Kinetic analysis of the reaction results suggests a Langmuir-type mechanism for the pure decalin, where the naphthalene adsorption causes inhibition. For mixtures, add to the product, solvent inhibition is also detected, especially in the case of aromatic ones (benzene and toluene) and on Pt/Al<sub>2</sub>O<sub>3</sub> catalyst.

Finally, the influence of decalin:methylcyclohexane vol./vol. ratio was deeply studied, observing that for Pt/C catalyst, 80:20 ratio is the most beneficial, so a compromise must be found between favoring the dissolution of naphthalene and the occupation of the catalytic centers by solvents that can compete with the own reagents of interest. From these results it is evidenced that a binary mixture of the potential LOHC with an saturated compound could improve its yield, which could be profit from the point of view of using aromatic compounds as LOHCs.

#### CRedit authorship contribution statement

**Eva Díaz:** . **Pablo Rapado-Gallego:** . **Salvador Ordóñez:** Supervision, Writing – review & editing, Funding acquisition.

#### Declaration of Competing Interest

The authors declare that they have no known competing financial interests or personal relationships that could have appeared to influence the work reported in this paper.

#### Data availability

Data will be made available on request.

#### Acknowledgements

Authors thanks the grant PID2020-112587RB-I00, BIOHYDROMER funded by AEI 10.13039/501100011033. Pablo Rapado acknowledges the Spanish Ministry of Education for the PhD grant that supports his research (PRE2021-097871).

#### References

- [1] A European Green Deal. Available online: [https://ec.europa.eu/info/strategy/priorities-2019-2024/european-green-deal\\_en](https://ec.europa.eu/info/strategy/priorities-2019-2024/european-green-deal_en) (accessed on 9 September 2021).
- [2] Sotoodeh F, Smith KJ. Structure sensitivity of dodecahydro-N-ethylcarbazole dehydrogenation over Pd catalysts. *J Catal* 2011;279:36–47. <https://doi.org/10.1016/j.jcat.2010.12.022>.
- [3] Briglevic B, Byum M, Lim H. Design, economic evaluation, and market uncertainty analysis of LOHC-based, CO<sub>2</sub> free, hydrogen delivery. *Appl Energy* 2020;274:115314. <https://doi.org/10.1016/j.apenergy.2020.115314>.
- [4] Preuster P, Papp P, Wasserscheid P. Liquid organic hydrogen carriers (LOHCs): Toward a hydrogen-free hydrogen economy. *Acc Chem Res* 2017;50:74–85. <https://doi.org/10.1021/acs.accounts.6b00474>.
- [5] Oh J, Bathula HB, Park JH, Suh Y. A sustainable mesoporous palladium-alumina catalyst for efficient hydrogen release from N-heterocyclic liquid organic hydrogen carriers. *Commun Chem* 2019;2:68. <https://doi.org/10.1038/s42004-019-0167-7>.
- [6] Martynenko EA, Vostikov SV, Pimerzin AA. Hydrogen production from decalin over silica-supported platinum catalysts: a kinetic and thermodynamic study. *React Kinet Mech Catal* 2021;133:713–28. <https://doi.org/10.1007/s11444-021-02037-1>.
- [7] Kalenchuk AN, Bogda VI, Dunaev SF, Kustov LM. Dehydrogenation of polycyclic naphthenes on a Pt/C catalyst for hydrogen storage in liquid organic hydrogen carriers. *Fuel Proc Tech* 2018;169:94–100. <https://doi.org/10.1016/j.fuproc.2017.09.023>.
- [8] Hydrogenious LOHC Technologies. <https://www.hydrogenious.net/index.php/en/hydrogen-2-2/> (Visited September 2022).
- [9] Hodoshima S, Arai H, Takaiwa S, Saito Y. Catalytic decalin dehydrogenation/naphthalene hydrogenation pair as a hydrogen source for fuel-cell vehicle. *Int J Hydrogen Energy* 2003;28:1255–62. [https://doi.org/10.1016/S0360-3199\(02\)00250-1](https://doi.org/10.1016/S0360-3199(02)00250-1).
- [10] Al-Muntaser AA, Varfolomeev MA, Suwaid MA, Saleh MM, Djimasbe R, Yuan C, et al. Effect of decalin as hydrogen-donor for in-situ upgrading of heavy crude oil in presence of nickel-based catalyst. *Fuel* 2022;313:122652.
- [11] Kim K, Oh J, Kim TW, Park JH, Han JW, Suh Y. Different catalytic behaviours of Pd and Pt metals in decalin dehydrogenation to naphthalene. *Catal Sci Technol* 2017;7:3728–35. <https://doi.org/10.1039/C7CY00569E>.
- [12] Kariya N, Fukuoka A, Utagawa T, Sakuramoto M, Goto Y, Ichikawa M. *App Catal A* 2003;247:247–59. [https://doi.org/10.1016/S0926-860X\(03\)00104-2](https://doi.org/10.1016/S0926-860X(03)00104-2).
- [13] Jiang N, Rao KSR, Jin M, Park S. Effect of hydrogen spillover in decalin dehydrogenation over supported Pt catalysts. *App Catal A* 2012;425–426:62–7. <https://doi.org/10.1016/j.apcata.2012.03.001>.
- [14] Lee G, Jeong Y, Kim B-G, Han JS, Jeong H, Na HB, et al. Hydrogen production by catalytic decalin dehydrogenation over carbon-supported platinum catalyst: Effect of catalyst preparation method. *Catal Commun* 2015;67:40–4.
- [15] Martynenko EA, Pimerzin AA, Savinov AA, Verevkin SP, Pimerzin AA. Hydrogen release from decalin by catalytic dehydrogenation over supported platinum catalysts. *Top Catal* 2020;63:178–86. <https://doi.org/10.1007/s11244-020-01228-9>.
- [16] Wang Y, Shah N, Huggins FE, Huffman GP. Hydrogen production by catalytic dehydrogenation of tetralin and decalin over stacked cone carbon nanotube-supported Pt catalysts. *Energy Fuels* 2006;20:2612–2625. <https://doi.org/10.1021/ef060228t>.
- [17] Kalenchuk AN, Smetneva DN, Bogdan VI, Kustov LV. Kinetics of decalin dehydrogenation on Pt/C catalyst. *Russ Chem Bull* 2015;64:2642–5. <https://doi.org/10.1007/s11172-015-1202-1>.
- [18] Wang B, Goodman DW, Froment GF. Kinetic modelling of pure hydrogen production from decalin. *J Catal* 2008;253:229–38. <https://doi.org/10.1016/j.jcat.2007.11.012>.
- [19] Faba L, Díaz E, Ordóñez S. Role of the support on the performance and stability of Pt-based catalysts for furfural-acetone adduct hydrodeoxygenation. *Catal Sci Technol* 2015;5:1473–84. <https://doi.org/10.1039/C4CY01360C>.
- [20] Kukula P, Červený L. The kinetics of methyl sorbate hydrogenation. *App Catal A* 1999;177:79–84. [https://doi.org/10.1016/S0926-860X\(98\)00258-0](https://doi.org/10.1016/S0926-860X(98)00258-0).
- [21] Faba L, Díaz E, Vega A, Ordóñez S. Hydrodeoxygenation of furfural-acetone condensation adducts to tridecane over platinum catalysts. *Catal Today* 2016;269:132–9.
- [22] Meemken F, Rodriguez-García L. Revealing catalytically relevant surface species by kinetic isotope effect spectroscopy: H-bonding to ester carbonyl of trans-ethyl pyruvate controls enantioselectivity on a cinchona-modified Pt catalyst. *J Phys Chem Lett* 2018;9:996–1001. <https://doi.org/10.1021/acs.jpcl.7b03360>.
- [23] Díaz E, McCall A, Faba L, Sastre H, Ordóñez S. Trichloroethylene hydrodechlorination in water using formic acid as hydrogen source: selection of catalyst and operation conditions. *Environ Prog Sustainable energy* 2012;32:1217–22. <https://doi.org/10.1002/ep.11730>.
- [24] Faba L, Díaz E, Ordóñez S. Hydrodeoxygenation of acetone-furfural condensation adducts over alumina-supported noble metal catalysts. *App Catal B* 2014;160–161:436–44. <https://doi.org/10.1016/j.apcatb.2014.05.053>.
- [25] Tuo Y, Jiang H, Li X, Shi L, Yu X, Li P. Kinetic behaviour of Pt catalyst supported on structured carbon nanofiber bed during hydrogen realising from decalin. *Int J Hydrogen Energy* 2016;6:10755–65. <https://doi.org/10.1016/j.ijhydene.2016.04.072>.
- [26] Li J, Tong F, Li Y, Liu X, Guo Y, Wang Y. Dehydrogenation of dodecahydro-N-ethylcarbazole over spinel supporting catalyst in a continuous flow fixed bed reactor. *Fuel* 2022;321:124034. <https://doi.org/10.1016/j.fuel.2022.124034>.
- [27] Wang J, Liu He, Fan S, Li W, Li Z, Yun H, et al. Size-dependent catalytic cyclohexane dehydrogenation with platinum nanoparticles on nitrogen-doped carbon. *Energy Fuels* 2020;34(12):16542–51.
- [28] Murzin DY. Kinetic analysis of cluster size dependent activity and selectivity. *J Catalysis* 2010;276:85–91. <https://doi.org/10.1016/j.jcat.2010.09.003>.
- [29] Sotoodeh F, Smith KJ. An overview of the kinetics and catalysis of hydrogen storage on organic liquids. *Canadian J of Chem Eng* 2013;91:1477–90. <https://doi.org/10.1002/cjce.21871>.

- [30] Kalenchuk AN, Kustov LM. Kinetic modelling of hydrogen production by dehydrogenation of polycyclic naphthalenes with varying degrees of condensation. *Molecules* 2022;27:2236. <https://doi.org/10.3390/molecules27072236>.
- [31] Dokjampa S, Rirksomboon T, Osuwan S, Jongpatiwut S, Resasco DE. Comparative study of the hydrogenation of tetralin on supported Ni, Pt and Pd catalysts. *Catal Today* 2007;123:218–23. <https://doi.org/10.1016/j.cattod.2007.01.004>.
- [32] Kalenchuk AN, Koklin AE, Bogdan VI, Kustov LM. Hydrogenation of naphthalene and anthracene on Pt/C catalysts. *Russ Chem Bull* 2018;67:1406–11. <https://doi.org/10.1007/s11172-018-2232-2>.
- [33] Pawelec B, Mariscal R, Navarro RM, van Bokhorst S, Rojas S, Fierro JLG. Hydrogenation of aromatics over supported Pt-Pd catalysts. *Appl Catal A* 2002; 225:223–37. [https://doi.org/10.1016/S0926-860X\(01\)00868-7](https://doi.org/10.1016/S0926-860X(01)00868-7).
- [34] Lin SD, Song C. Noble metal catalysts for low-temperature naphthalene hydrogenation in the presence of benzothiophene. *Catal Today* 1996;31:93–104. [https://doi.org/10.1016/0920-5861\(96\)00038-7](https://doi.org/10.1016/0920-5861(96)00038-7).
- [35] Kwak Y, Moon S, Ahn C-i, Kim A-R, Park Y, Kim Y, et al. Effect of the support properties in dehydrogenation of biphenyl-based eutectic mixture as liquid organic hydrogen carrier (LOHC) over Pt/Al<sub>2</sub>O<sub>3</sub> catalysts. *Fuel* 2021;284:119285.
- [36] Kalenchuk A, Bogdan V, Dunaev S, Kustov L. Influence of steric factors on reversible reactions of hydrogenation-dehydrogenation of polycyclic aromatic hydrocarbons on a Pt/C catalyst in hydrogen storage systems. *Fuel* 2020;280: 118625. <https://doi.org/10.1016/j.fuel.2020.118625>.
- [37] Díaz E, Rapado-Gallego P, Ordóñez S. Systematic evaluation of physicochemical properties for the selection of alternative liquid organic hydrogen carriers. *J Energy Storage* 2023;59:106511. <https://doi.org/10.1016/j.est.2022.106511>.
- [38] Shafaghat H, Rezaei PS, Daud WMAW. Using decalin and tetralin as hydrogen source for transfer hydrogenation of renewable lignin-derived phenolics over activated carbon supported Pd and Pt catalysts. *J Taiwan Inst Chem Eng* 2016;65: 91–100. <https://doi.org/10.1016/j.jtice.2016.05.032>.
- [39] Ali LI, Ali AA, Aboul-Futouh SM, Aboul-Gheit AK. Dehydrogenation of cyclohexane on catalysts containing noble metals and their combinations with platinum on alumina support. *Appl Catal A* 1999;177:99–110. [https://doi.org/10.1016/S0926-860X\(98\)00248-8](https://doi.org/10.1016/S0926-860X(98)00248-8).
- [40] Kyzas GZ, McKay G, Al-Musawi TJ, Salehi S, Balarak D. Removal of benzene and toluene from synthetic wastewater by adsorption onto magnetic zeolitic imidazole framework nanoparticles. *Nanomaterials* 2022;12:3049. <https://doi.org/10.3390/nano12173049>.